Coupling of Non-Equilibrium Green's Function and Wigner Function Approaches

O. Baumgartner, P. Schwaha, M. Karner, M. Nedjalkov, and S. Selberherr
Institute for Microelectronics, TU Wien
E-mail: {baumgartner|schwaha|karner|nedjalkov|selberherr}@iue.tuwien.ac.at
Gußhausstraße 27–29/E360, A-1040 Wien, Austria

***Abstract*—We propose a coupling scheme, where the advantages of the coherent Green's function formalism are combined with the ability of the Wigner formalism to account for phase-breaking processes of interaction with phonons and other lattice imperfections. The Green's function formalism is used to calculate the coherent Wigner function which provides the initial condition in an equation, from which corrections due to phonon interactions can be calculated. A variety of possible approaches to the obtained equation are considered, and the case where the initial condition is small is investigated numerically.**

I. INTRODUCTION

The nano-era of semiconductor devices involves novel materials and architectures, along with length scales of the channel, gate, screening and scattering lengths, which begin to become comparable to one another. A number of novel phenomena govern the device behavior, which must be taken into account in the simulation models. While some of them can be described in classical terms, others, being dominant at nanometer and femtosecond scales, require a quantum description. Coherent processes such as quantization and tunneling have been in the research scope since more than two decades using the Green's function formalism [1](and the references therein), or the Wigner function [2]. Further efforts are devoted to exploring the role of incoherent phenomena due to interactions with phonons and other lattice imperfections. These phase-breaking processes affect the carrier momentum, which, additionally, has an effect on the electrostatics due to the change of the carrier density distribution. It has recently been demonstrated, within a Green's function formalism, that the scattering near barriers affects the transport by changing the carrier density, which in turn modifies the potential profile via the Poisson equation [3]. Due to this effect the phonon scattering near the drain end in a MOSFET influences the drain current, if the channel length is comparable to the scattering length, in contrast to long channel devices. It has furthermore been shown that self-consistent Wigner function simulations of double gate (DG) MOSFETs, which account for phonon interaction via the Boltzmann scattering model, can successfully bridge the gap between purely coherent and scattering-dominated (classical) transport conditions [4]. We suggest an alternative transport model here which is based on the advantages of both formalisms.

II. COHERENT TRANSPORT

The non-equilibrium Green's function (NEGF) approach offers the most comprehensive, self-consistent way to account for both coherent space/time correlations and incoherent processes [5]. The system is open via the coupling of the quantum region with the contact self-energies, while dissipation is introduced via the scattering self-energies. However, due to the latter the method becomes computationally expensive when compared with the coherent counterpart. Just the opposite situation is encountered with the Wigner function approach which can easily account for phase breaking processes utilizing the Boltzmann scattering models.

In the suggested scheme stationary, coherent Green's function simulations provide the density matrix $\rho(x,x')$ as obtained from the lesser Green's function

$$\rho(x,x') = -2\imath \int G^<(x,x',\mathcal{E})\frac{d\mathcal{E}}{2\pi}.$$

$$G^<(x,x',\mathcal{E}) = G^R(x,x',\mathcal{E})\Sigma^<(x,x',\mathcal{E})G^A(x,x',\mathcal{E}),$$

$$G^R(x,x',\mathcal{E}) = [\mathcal{E}I - H(x,x',\mathcal{E}) - \Sigma^R(x,x',\mathcal{E})]^{-1}.$$

$$G^R(x,x',\mathcal{E}) = G^{A\dagger}(x,x',\mathcal{E})$$

with the usual notations for the retarded and advanced $G^{R,A}$ counterparts, the $\Sigma^{<,R}$ are the corresponding self-energies and $H(x,x',\mathcal{E})$ is the Hamiltonian. Within the self-consistent Schrödinger-Poisson loop a recursive Green's function algorithm [6] has been employed to reduce computational costs. After thereby obtaining the conduction band edge, a full Green's function calculation yields the density matrix. Additionally, an adaptive energy integration scheme [7] has been applied to correctly resolve narrow resonances and ensure numerical accuracy.

The density matrix can be used to obtain the coherent Wigner function

$$f_w^c(x,k_x) = \frac{1}{2\pi}\int ds e^{-ik_x s}\rho(x+\frac{s}{2},x-\frac{s}{2});$$

where $x = \frac{x_1+x_2}{2}$, $s = x_1 - x_2$. Furthermore f_w^c is a solution of the coherent part of the Wigner-Boltzmann equation

$$\frac{\hbar k_x}{m}\frac{\partial}{\partial k_x}f_w^c(x,k_x) = \int dk_x' V_w(x,k_x'-k_x)f_w^c(x,k_x') \qquad (1)$$

where V_w is the Wigner potential.

978-1-4244-1753-7/08/$25.00 ©2008 IEEE

III. SCATTERING CORRECTION

The Wigner equation for a one-dimensional stationary transport problem is:

$$\frac{\hbar k_x}{m}\frac{\partial}{\partial x}f_w(x,\mathbf{k}) = \int dk_x' V_w(x,k_x'-k_x)f_w(x,k_x',\mathbf{k}_{yz}) + \int d\mathbf{k}' f_w(x,\mathbf{k}')S(\mathbf{k}',\mathbf{k}) - f_w(x,\mathbf{k})\lambda(\mathbf{k}) \quad (2)$$

Here phase-breaking processes are accounted for by the Boltzmann scattering operator with $S(\mathbf{k},\mathbf{k}')$ the scattering rate for a transition from $\mathbf{k}$ to $\mathbf{k}'$ and $\lambda(\mathbf{k}) = \int d\mathbf{k}' S(\mathbf{k}.\mathbf{k}')$ the total out-scattering rate. Equation (1) can be obtained from Equation (2) by setting the scattering rate S (and thus λ) to zero. In this case the $\mathbf{k}_{yz}$ dependence remains arbitrary, and can be specified via the boundary conditions. Formally, the extrapolation must be such that $f_w^c(x,k_x')$ is recovered when integrating over $\mathbf{k}_{yz}$. Moreover, we want the Boltzmann scattering operator at the boundaries to cancel, where standard equilibrium conditions are assumed. Therefore, a Maxwell-Boltzmann distribution $f_{MB}(k_{yz}')$ is assumed in the yz-directions, and the function:

$$f_w^c(x,\mathbf{k}') = f_w^c(x,k_x')\frac{\hbar^2}{2\pi mkT}e^{-\hbar^2(k_y'^2+k_z'^2)/2mkT}$$

can be introduced. We are interested to obtain an equation for the correction $f_w^\Delta(x,k_x,\mathbf{k}_{yz}) = f_w(x,\mathbf{k}) - f_w^c(x,\mathbf{k})$. The following steps are suggested: Equation (1) is multiplied by $f_{MB}(x,k_{yz})$ and subtracted from Equation (2). f_w^Δ appears in the Boltzmann terms by adding and subtracting the counterparts with f_w^c. Finally, an integral form is obtained with the help of trajectories $X(t) = x + v_x(k_x)t$:

$$f_w^\Delta(x,\mathbf{k}) = \int_0^{t_b} dt \Big\{ \int dk_x' V_w(X(t),k_x'-k_x) f_w^\Delta(X(t),k_x',\mathbf{k}_{yz}) e^{-\lambda(\mathbf{k})t} + \int d\mathbf{k}' S(\mathbf{k}',\mathbf{k}) e^{-\lambda(\mathbf{k})t} f_w^\Delta(X(t),\mathbf{k}') + \int d\mathbf{k}' S(\mathbf{k}',\mathbf{k}) e^{-\lambda(\mathbf{k})t} f_w^c(X(t),\mathbf{k}') - f_w^c(X(t),\mathbf{k})\lambda(\mathbf{k}) e^{-\lambda(\mathbf{k})t} \Big\} \quad (3)$$

t_b is the time needed for a trajectory $X(t)$ initialized by (x,k_x) to reach the boundary of the device. We note that f_w^Δ becomes zero at the boundaries as the boundary conditions are the same in the two cases.

IV. DISCUSSION

The last row of the derived second order Fredholm integral equation is the free term $f_w^{\Delta,0}$, which can be interpreted as an initial condition determined by the function f_w^c. The correction f_w^Δ can be expanded into a Neumann series, obtained by consecutive iterations of the equation into itself. The terms in the expansion account for the correlations between the two components of the kernel, the Wigner potential and the scattering operators.

The obtained equation is exact in the sense that there are no approximations introduced during the process of derivation: it is equivalent to solve Equation (2), or to know f_w^c and to solve Equation (3), which can be solved by any of the existing Wigner particle approaches [4], [8]. Certain advantageous numerical properties are related to the following: An initial condition problem is considered, with an evolution directed from within the device to the boundaries. The solution is expected to be small with respect to the coherent counterpart, because for usual applications the Wigner potential is of order $10^{15-16} sec^{-1}$, while the Boltzmann operator is two orders of magnitude smaller. Nevertheless the computational efforts related to quantum-particle methods are significant, so that some approximations can be suggested depending on the physical situation. First, the approach proposed by Gehring and Kosina [9] of decomposing the Wigner potential into classical and quantum parts can be utilized. Alternatively, a local field approximation of the Wigner potential in Equation (3) transforms the equation into the classical Boltzmann equation. Moreover, close to almost coherent transport conditions $f_w^{\Delta,0}$ may already be sufficiently small, so that physical averages can be obtained by using $(f_w^{\Delta,0} + f_w^c)$. In all cases the solution of Equation (3) or its approximations lead to a redistribution of the charge density. Figure 1 presents a scheme inspired by the results of Svizhenko [3], who demonstrated the importance of effects due to the interplay of electrostatics and scattering of the current carriers in small devices. A self-consistent loop between the NEGF and the Wigner correction simulators accounts for the change of the density due to scattering.

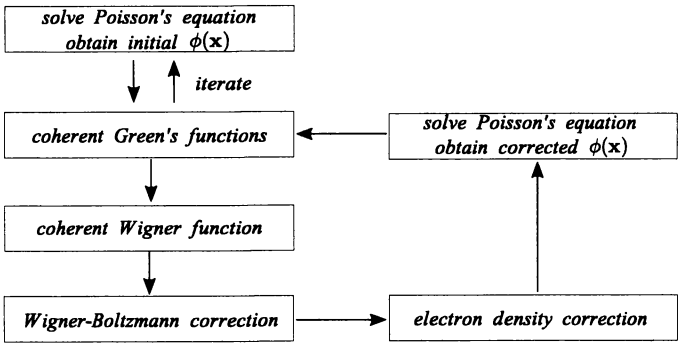

Fig. 1: Iteration scheme.

The computation of the initial condition is a necessary step in all of the considered approaches. In the following, we discuss the Monte Carlo method devised for evaluation of $f_w^{\Delta,0}$ and explore relevant physical conditions where the correction term is sufficiently small.

V. STOCHASTIC APPROACH

The value of $f_w^{\Delta,0}$ given by the last row of Equation (3) is obtained by computing the two integrals separately using two Monte Carlo algorithms. We additionally integrate over k_y, k_z which is relevant for one-dimensional devices. The integrands are decomposed into products of conditional probability densities which give rise to free-flight and scattering events.

The values of the second integral, can be evaluated point wise. For a given input point x, k_x we select k_y, k_z with a proba-

bility distribution given by Maxwell-Boltzmann statistics. This determines the value of $\lambda(\mathbf{k})$. The latter is used in the exponent to select the flight time t by applying the standard algorithm for device Monte Carlo simulators. The selected variables allow to evaluate $f_w^c(x+v_x(k_x)t,k_x)$ which is accumulated into a Monte Carlo estimator. Usually f_w^c is known on a grid point, so that the function is assumed point wise constant. The value of the second integral in the input point is obtained by dividing the estimator by the number of trajectories.

The first integral can be evaluated point wise only by a backward algorithm. A forward one gives the values averaged around the points of the grid. The initial point of a trajectory is selected randomly in accordance with the values of f_w^c. A scattering event occurs with a probability determined by S, with the free flight time selected using the after-scattering values of the wave vector. The current trajectory terminates and the estimator accounts for the ratio of the out-scattering rates of the before- and after- scattering states and furthermore the sign of the initial f_w^c. The algorithm then continues by constructing a new trajectory.

We note that a high precision is achieved in contrast to the usual distribution function simulations where the whole iterative series of the Boltzmann equation is computed.

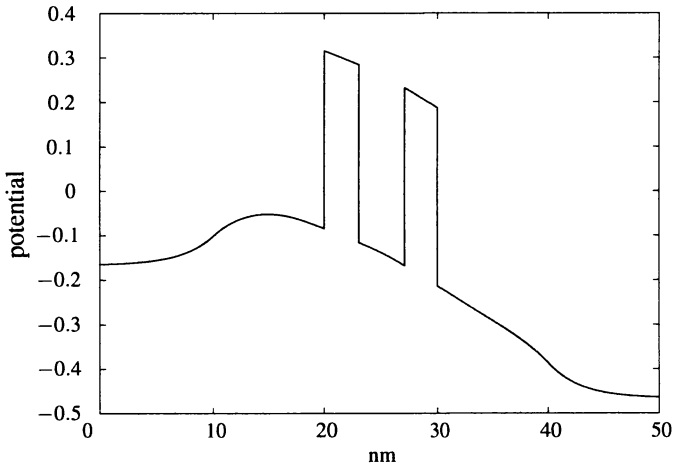

Fig. 2: RTD potential profile.

VI. SIMULATIONS

We present simulation results for resonant-tunneling devices. Standard GaAs material parameters are used and only the Gamma valley is considered. The scattering rate S accounts for interactions with the three-dimensional acoustic, deformation potential and optical phonons.

Figure 2 shows the potential of an RTD device with $3nm$ barriers surrounding a $4nm$ well. $0.3V$ bias is applied. The device is surrounded by a $10nm$ highly doped contact $5.10^{18}cm^{-3}$ and $10nm$ low doped region $10^{17}cm^{-3}$. The height of the barriers is $0.4eV$. Figure 3 shows the corresponding Wigner function f_w^c as obtained from the NEGF density matrix by using a coherence length of $50nm$. The device region has the same length, and the density matrix is computed in a quantum region spread by $\pm 25nm$ around the device. The accumulation region inside the well and the oscillatory behavior around the barriers are well distinguished, which demonstrates that the chosen values of the parameters are appropriate.

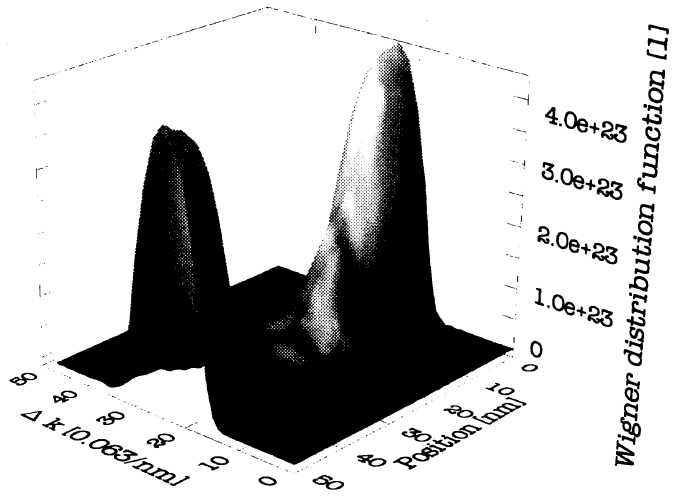

Fig. 3: Wigner distribution function.

An important condition for the relevance of the method is discussed: The two integrals must coincide at the ends of the simulation region since $f_w^{\Delta,0}$ must become zero at the boundaries. If NEGF simulations with Fermi-Dirac statistics are utilized, this leads to an offset of the densities at the boundary points as shown in Figure 4.

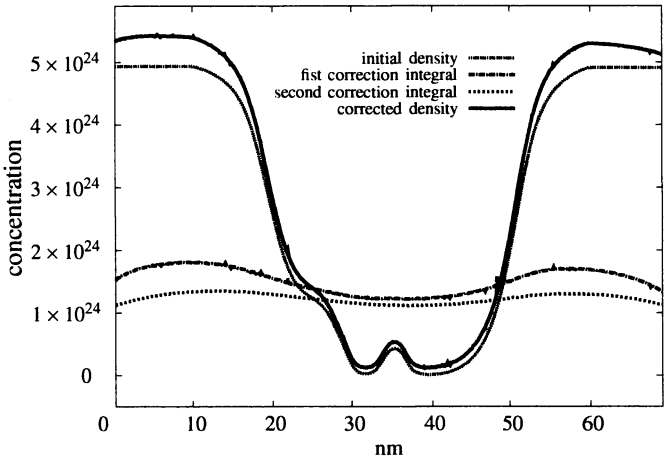

Fig. 4: Density offset at the boundaries due to inconsistent boundary conditions.

Figure 5 is the counterpart to Figure 4 using Maxwell-Boltzmann statistics. The two integrals coincide in the boundary regions, and the correction of the density is small in the rest of the device. Unfortunately the corrected density becomes

negative in the regions inside the barriers. We associated this peculiarity with the oscillations of f_w^c, which are typical for these regions. To verify this assumption we conducted further experiments with the height and thickness of the barriers, the length of the well, and with similar device with graded barriers. Appearance of the negative densities persisted in all experiments and can cover the whole active region if the latter is very small. We concluded that in these cases the zeroth order correction, despite small, is not sufficient for an adequate approximation and higher order terms in the Neumann expansion of Equation (3) must be considered.

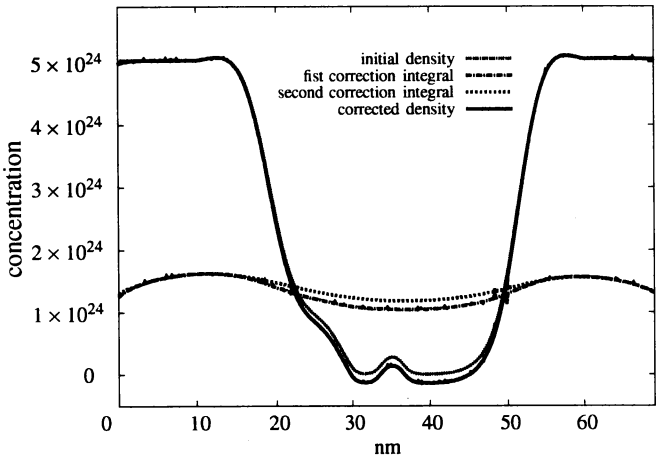

Fig. 5: Density distribution obtained with correct boundary conditions.

The correction for terms have also been calculated for a second RTD similar to the previous device, but with $1nm$ barriers surrounding a $4nm$ well embedded in a $6.5nm$ highly doped contact $5.10^{18}cm^{-3}$ and $2.0nm$ low doped region $1.10^{17}cm^{-3}$. The height of the barriers is $0.3eV$. The results for this shorter device indicate, that the situation of only using the zeroth order correction improves.

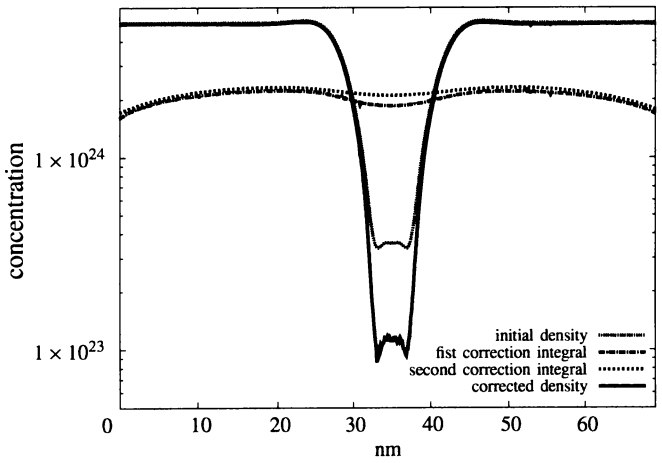

Fig. 6: Density distribution in the second device without bias, presented in logarithmic scale.

The contacts of this device with $25nm$ are actually closer compared to the previous case. The corrected density, shown in Figure 6, does not have areas with negative values and thus the initial condition can already be accepted as a relevant zeroth order correction.

Applying bias to the structure does not disturb the validity of the obtained correction, as can be seen in Figure 7.

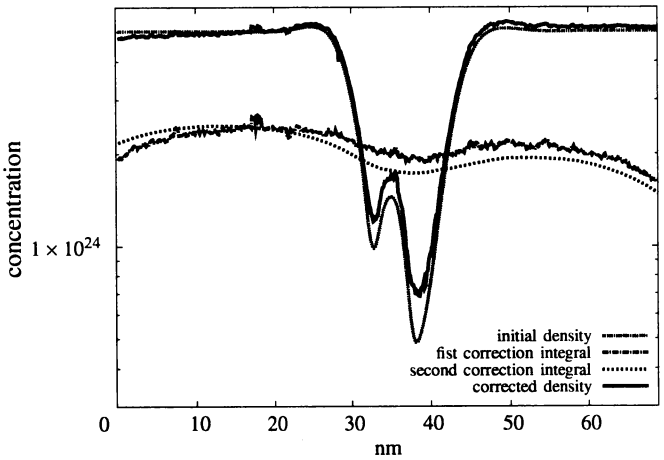

Fig. 7: Density distribution in the second device under $0.3V$ bias, presented in logarithmic scale.

VII. CONCLUSION

An equation for the phonon scattering induced correction to the coherent Wigner function has been derived. The coherent function, computed by using a NEGF technique, provides the initial condition for this equation. The equation can be solved directly by existing Wigner simulators, or, depending on the physical situation, can be approximated. In all cases the explicit knowledge of the initial condition is needed. A Monte Carlo method is suggested for this purpose. The peculiarities of the correction are explored numerically for the case of RTD devices.

ACKNOWLEDGMENT

This work has been partially supported by the Österreichische Forschungsgemeinschaft (ÖFG), Project MOEL273 and by the Austrian Science Fund, special research program IR-ON (F2509).

REFERENCES

[1] S. Datta, Superlattices & Microstructures **28**, 253 (2000).
[2] N. C. Kluksdahl *et al.*, Physical Review B **39**, 7720 (1989).
[3] A. Svizhenko and M. P. Antram, IEEE Trans. on Electron Devices **50**, 1459 (2003).
[4] D. Querlioz *et al.*, IEEE Trans. on Nanotechnology **5**, 737 (2006).
[5] R. Lake and S. Datta, Physical Review B **45**, 6670 (1992).
[6] A. Svizhenko *et al.*, J. Appl. Phys. **91**, 2343 (2002).
[7] O. Baumgartner *et al.*, in *Technical Proceedings of the 2007 NSTI Nanotechnology Conference* (2007), Vol. 3, pp. 145–148.
[8] M. Nedjalkov *et al.*, Physical Review B **70**, 115319 (2004).
[9] A. Gehring and H. Kosina, Journal of Computational Electronics **4**, 67 (2005).